Technical University of Denmark

DTU

Oxidation and reduction kinetics of eutectic SnPb, InSn, and AuSn: a knowledge base for fluxless solder bonding applications

Kuhmann, Jochen Friedrich; Preuss, A.; Adolphi, B.; Maly, K.; Wirth, T.; Oesterle, W.; Pittroff, W.; Weyer, G.; Fanciulli, M.

DTU Library
Technical Information Center of Denmark

Oxidation and Reduction Kinetics of Eutectic SnPb, InSn, and AuSn: A Knowledge Base for Fluxless Solder Bonding Applications

Jochen F. Kuhmann, Andrea Preuss, Barbara Adolphi, Karsten Maly, Thomas Wirth,
Werner Oesterle, Wolfgang Pittroff, Gerd Weyer, and Marco Fanciulli

Abstract— For microelectronics and especially for upcoming new packaging technologies in micromechanics and photonics fluxless, reliable and economic soldering technologies are needed. In this article, we consequently focus on the oxidation and reduction kinetics of three commonly used eutectic solder alloys:

1) SnPb;
2) InSn;
3) AuSn.

The studies of the oxidation kinetics show that the growth of the native oxide, which covers the solder surfaces from the start of all soldering operations is self-limiting. The rate of oxidation on the molten, metallic solder surfaces is significantly reduced with decreasing O_2 partial-pressure. Using *in situ* Auger electron spectroscopy (AES) it could be shown for the first time, that H_2 can reduce Sn-oxide as well as In-oxide at moderate heating duration and temperatures.

In the second part of this study, the results, obtained by the investigation of oxidation and reduction kinetics, are applied to flip-chip (FC) bonding experiments in vacuum with and without the injection of H_2. Wetting in vacuum is excellent but the self-alignment during flip-chip soldering is restricted. The desired, perfectly self-aligned FC-bonds have been only achieved, using evaporated and reflowed AuSn(80/20) and SnPb(60/40) after the introduction of H_2.

Index Terms— Auger electron spectroscopy, AuSn, flip-chip bonding, fluxless soldering, InSn, oxidation kinetics, SnPb.

I. INTRODUCTION

FLUXLESS soldering has been a topic for many researchers in the last decade. Environmental concerns and reliability issues have been the main drive [1]–[3]. In the last few years, other topics appeared which again increased the impetus to develop fluxless soldering techniques: The assembly of micromachined [4], [5] and photonic devices [6], [7] and low cost flip-chip (FC) solder bonding on organic substrate materials [8], [9].

In the case of micromachined components, fluxes can clog nozzles and air gaps and destroy very thin and sensitive membranes. Cleaning of fluxes in order to remove corrosive flux residues will be aggravated by capillary forces and might in the case of sensors with membranes not be tolerable at all. For the photonic assembly the major concern in using fluxes is attenuation or deflection of the optical signal and degradation of unpassivated devices. The need to use underfiller in order to compensate for the higher thermal mismatch between organic substrates and silicon dies are the main driving forces in the area of low cost, high volume application. Here the residues of fluxes can lead to poor adhesion of the underfiller and subsequently to failure of the joint when subjected to thermal cycling.

Despite all efforts to circumvent the use of fluxes for sensitive applications too little is known about solder oxides, their growth during soldering in ambient and under reduced O_2 partial-pressures. In addition, the potential of H_2 to reduce oxides on solder surfaces at typical bonding temperatures is misconceived [10]–[12]. Therefore, in this article we present both new and previously published data about fluxless, self-aligned FC-solder bonding investigations [13]–[16] together with the study of oxidation and reduction kinetics on eutectic InSn [17], SnPb [18], and AuSn.

The studies to determine the scale growth of the oxide were carried out using Auger electron spectroscopy (AES). The thickness of the films, formed on eutectic InSn and SnPb were measured as a function of temperature and O_2 partial-pressure. In the case of SnPb(60/40) the native oxide layer was additionally characterized using Moessbauer spectoscropy (MS) and transmission electron microscopy (TEM).

Furthermore, for all solders the results of *in-situ* AES measurements will be given, which prove the potential of H_2 to reduce the solder oxides. The applicability of H_2 as an effective flux substitute during bonding at moderate temperatures and heating cycles will be demonstrated by photographs, recorded during FC-bonding experiments.

II. OXIDATION AND REDUCTION IN VACUUM

A. Thermodynamics of Oxidation

The change in the Gibbs free energy ΔG, associated with a chemical reaction gives the answer, whether a reaction as, e.g., the oxidation of tin (1) will ($\Delta G < 0$) or will not occur ($\Delta G > 0$).

TABLE I
VALUES OF THE STANDARD GIBBS FREE
ENERGY ΔG^0 FOR THE RELEVANT OXIDES[19]

T (°C)	ΔG^0 (10^5 J/mol)				
	SnO	SnO$_2$	In$_2$O$_3$	PbO	PbO$_2$
150	-4.9	-4.93	-8.3	-3.54	-2
200	-4.82	-4.83	-8.06	-3.44	-1.91
250	-4.74	-4.74	-7.9	-3.43	-1.81
300	-4.64	-4.63	-7.74	-3.24	-1.72
350	-4.54	-4.52	-7.57	-3.14	

TABLE II
VALUES OF p_{H_2}/p_{H_2O} PARTIAL-PRESSURE RATIOS
FOR THERMODYNAMIC EQUILIBRIUM ($\Delta G = 0$)

T (°C)	p_{H_2}/p_{H_2O}				
	SnO	SnO$_2$	In$_2$O$_3$	PbO	PbO$_2$
150	590	840	$1.3 \ 10^5$	$2 \ 10^{-6}$	$7 \ 10^{-16}$
200	170	210	$9.2 \ 10^3$	$5 \ 10^{-6}$	$1 \ 10^{-14}$
250	82	80	$3.5 \ 10^3$	$8 \ 10^{-6}$	$2 \ 10^{-13}$
300	35	31	10^3	10^{-5}	$1 \ 10^{-12}$
350	16	13	226	$2 \ 10^{-5}$	

The following equations exemplify the thermodynamic calculations for the oxidation of tin to stannic oxide

$$Sn + O_2 = SnO_2. \tag{1}$$

Whether oxidation or decomposition of the oxide occurs is determined by the Gibbs free energy ΔG^0 at the relevant temperature. For equilibrium condition ($\Delta G = 0$) ΔG^0 is given by

$$\Delta G^0 = RT \ln(k_p) \tag{2}$$

in which R is the molar gas constant and k_p the equilibrium constant. Equation (2) can also be expressed in terms of O$_2$ partial-pressure (p_{O_2}), normalized by the O$_2$ partial-pressure under standard conditions ($p_{O_2}^0$) as

$$\Delta G^0 = RT \ln \left(\frac{p_{O_2}}{p_{O_2}^0} \right). \tag{3}$$

P_{O_2} at 250 °C for the oxidation of Sn to stannic oxide as described in (1) is given as

$$p_{O_2} = 10^{-43} \text{ Pa.} \tag{4}$$

Partial-pressures in this range can clearly not be realized by vacuum equipment. Therefore a chemical reaction is used to reach O$_2$ partial-pressures in that order of magnitude

$$2H_2 + O_2 \rightleftharpoons 2H_2O(g). \tag{5}$$
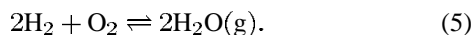
According to (2) the equilibrium constant k_p of water formation (5) at a specific temperature defines the O$_2$ partial-pressure as

$$P_{O_2} = \frac{p(H_2O)^2}{k_p \cdot p(H_2)^2}. \tag{6}$$

From a thermodynamic point of view Sn should be predominantly oxidized in AuSn and SnPb solders whereas in InSn alloys In would be oxidized preferentially. Table I gives an overview of the available ΔG^0 values for the possible oxides. Table II lists the p_{H_2}/p_{H_2O} which mark the threshold between oxide formation and decomposition ($\Delta G = 0$).

It is of great importance to realize that meeting the boundary conditions for reduction is mandatory in order to reduce the oxide layers. This means, that the ambient needs to be very well controlled. The desorption of water during heating or contamination of the solder stemming from photoresist or co-deposits during electroplating have a detrimental effect on the reduction. These are the reasons why we believe the potential of H$_2$ to reduce Sn-oxide has been misjudged as stated before.
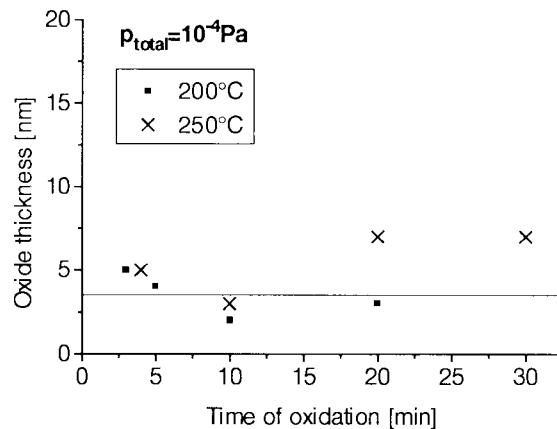

Fig. 1. Scale growth on liquid nonreduced samples during 10^{-4} Pa at 200 and 250 °C.

B. Oxidation Kinetics

The oxide growth on eutectic SnPb and InSn was investigated by means of AES. For InSn(51.2/48.8) the starting point of the measurement was always the metallic, sputtered surface whereas in the case of SnPb(60/40) some samples were still covered by their native oxide, grown during storage at room temperature.

1) SnPb(60/40): The native oxide of SnPb(60/40) was measured to have a thickness of approximately 3.5 nm, regardless of the storage times between three days and three months. Some samples which were heat treated showed an erratic growth which was contributed to spallation of the oxide layers. The samples which were heat-treated in vacuum ($p_{total} = 10^{-4}$ Pa) and ambient at 200 and 250 °C showed no or very little increase in oxide thickness (Figs. 1 and 2).

The lines in Figs. 1 and 2 depict the thickness of the native oxide. In contrast to that, the samples which were reduced by H$_2$ (2 min, 250 °C at H$_2$/H$_2$O $\geq$ 100) prior to oxidation, exhibited in the investigated time range of 3 to 30 min a significant scale growth of up to 40 nm in thickness. To guide the eye, the scale growth in Figs. 3–5 was fitted to a time-to-the-square-root law. The growth of the scales showed a dependence on temperature (Fig. 3) as well as on O$_2$ partial-pressures (Figs. 4 and 5).

The native oxide and the oxide grown on the molten, metallic surface at 250 °C have been investigated by TEM. Electron diffraction patterns and EDX spectra identified the oxide, grown on the liquid solder as polycrystalline SnO. The
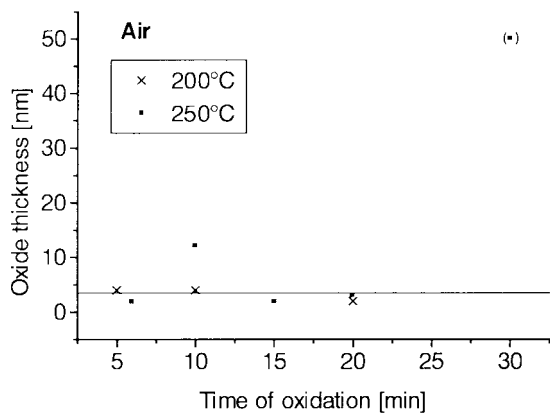
Fig. 2.   Scale growth on liquid nonreduced samples during heating in air at 200 and 250 °C.
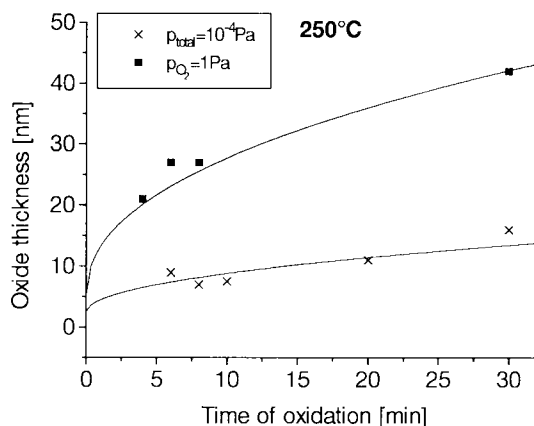

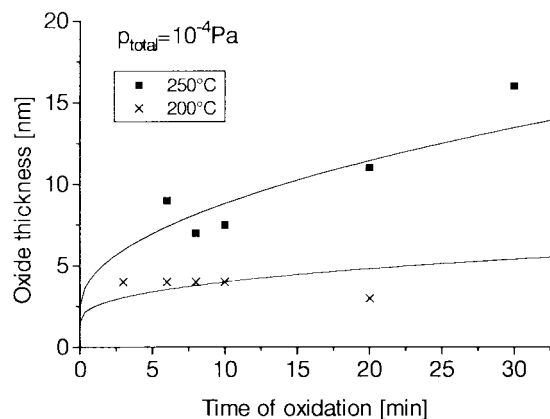Fig. 3.   Scale growth on liquid SnPb(60/40) during 10^{-4} Pa at 200 and 250 °C.

Fig. 4.   Scale growth on liquid SnPb(60/40) during different pressures at 200 °C.

films carrying the native oxide did not yield any diffraction patterns but could neither be characterized by EDX. Moessbauer Spectroscopy was therefore carried out to determine the binding state within the native oxide: with this method the oxide could be identified unambiguously as SnO_2. No stannous oxide was detected.

2) InSn(51.2/48.8): Eutectic InSn was oxidized at 22, 100, 150, and 250 °C. For the oxidation treatment at 4×10^{-8}, $7\times$

Fig. 5.   Scale growth on liquid SnPb(60/40) during different pressures at 250 °C.

Fig. 6.   Scale growth on eutectic InSn during different O_2 partial-pressures at 22 °C.

10^{-5}, 7×10^{-4} Pa partial-pressure of O_2, which was carried out inside the AES chamber, the samples were sputtered prior to oxidation to remove the native oxide. This was not possible for the samples treated in ambient (O_2 partial-pressure $= 2\times 10^4$ Pa). Here the native oxide was left on top of the samples. Figs. 6–9 give the measured scale growth of the samples as a function of O_2 partial-pressure and temperature. The scale growth of the samples treated below the melting point of the solder (120 °C) could be fitted to a logarithmic law whereas above the melting point of the solder a parabolic growth law was observed.

The characterization of the oxide films were carried out by X-ray diffraction (XRD) and X-ray photon spectoscropy (XPS). Despite the intermetallic phases $InSn_4$ and In_3Sn no oxide was found on the samples which have been stored at room temperature. On samples treated at temperatures above the melting point In_2O_3, $In(OH)_3$, SnO, and SnO_2 were detected by XRD.

XPS of samples treated at room temperature and at 190 °C showed the surfaces to have a similar composition of the oxide: In_2O_3, In_2O, SnO, and with increasing depth also metallic In and Sn. A distinct surface segregation of In, which increased with increasing temperature, could be found on all the investigated samples.
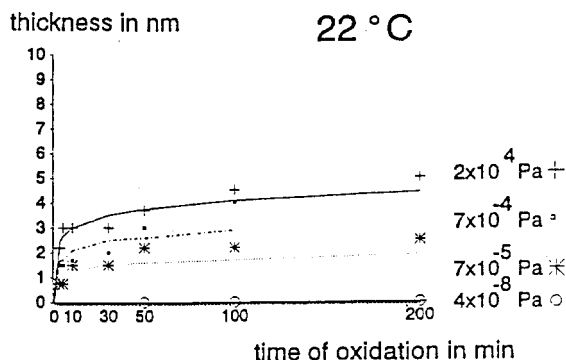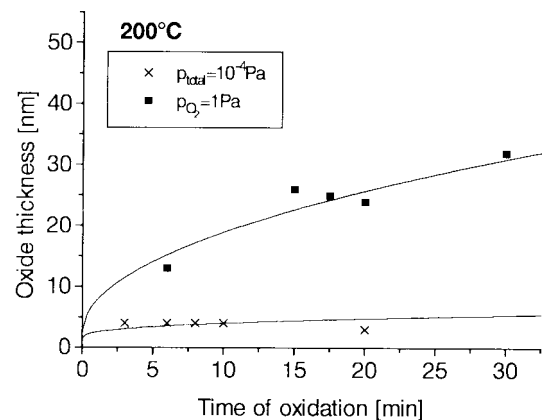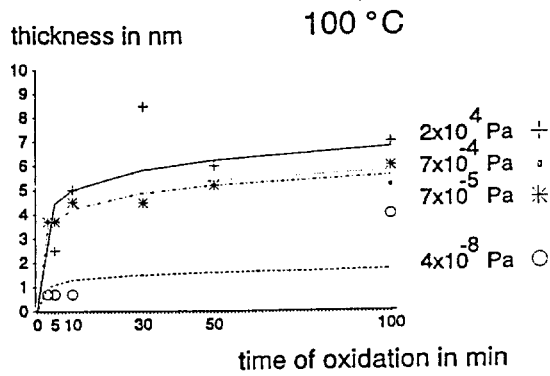
Fig. 7.   Scale growth on eutectic InSn during different O_2 partial-pressures at 100 °C.
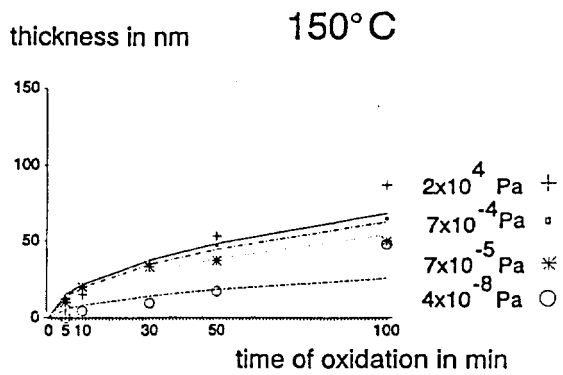

Fig. 8.   Scale growth on eutectic InSn during different O_2 partial-pressures at 150 °C.
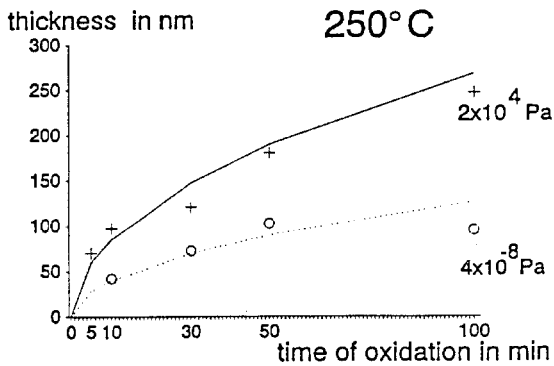

Fig. 9.   Scale growth on eutectic InSn during different O_2 partial-pressures at 250 °C.

3) AuSn(80/20): AuSn samples were only characterized as to their native oxide. Similar to eutectic SnPb and InSn also AuSn exhibits a difference between surface and bulk concentration of the solder: Sn segregates to the surface and is, of course, the only element to be oxidized in this solder. By AES the oxide covering eutectic AuSn was found to have approximately the same thickness as the oxide which is covering eutectic SnPb ($\sim$3 nm).
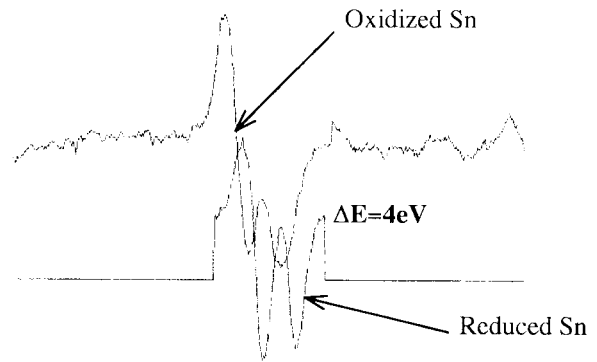

Fig. 10.   Energy shift during *in situ* AES between Sn-oxide and metallic tin, observed during reduction of oxides on eutectic SnPb and AuSn by H_2 at 240 °C.

C. Reduction

Reduction experiments were carried out for all three solders by *in situ* AES. Sn and In, which are the predominantly oxidized species in the investigated alloys, have a distinct energy difference of several eV between the oxidized and the metallic state spectra. The reduction was therefore monitored by this energy shift. The thermodynamical conditions for the decomposition of the oxide at temperatures relevant for soldering operations are given in Table II. The samples, covered with their native oxide were introduced into the AES chamber which was then pumped down to 10^{-9} Pa. This pressure was estimated conservatively to consist mainly of the H_2O partial-pressure. Then the samples were heated up and H_2 was introduced, allowing the pressure to augment the initial base pressure by the factors given in Table II. The typical AES spectra of tin peaks in SnPb(60/40) and AuSn(80/20) before and after treatment with H_2 can be seen in Fig. 10. At approximately 250 °C a distinct energy shift was observed between the oxidized and metallic state of tin. The energy shift was recorded within 2 min. It is interesting to note that the reduction of Sn-oxide on AuSn(80/20) occurred, while the solder was still solid.

Fig. 11 describes the reduction of In-oxide by H_2. In_2O_3 is much more stable than SnO or SnO_2 and therefore also higher H_2/H_2O ratios are required. This is the reason, why in the case of this solder alloy the temperature needed to be elevated to 250 °C in order to meet the required thermodynamic boundary conditions (see Table II).

III. REFLOW AND BONDING EXPERIMENTS

Reflow experiments with solder bumps of all three investigated materials were done in vacuum. Very smooth bumps with the desired shape of a truncated sphere were obtained when using SnPb and also AuSn (see Fig. 12). In both cases the solder material was deposited by evaporation technologies. In the case of eutectic InSn the bumps were deposited by electroplating. The surface as well as the homogeneity of the electroplated InSn solder bumps was of lower quality compared to the material, deposited by evaporation (see Fig. 13).

Bonding experiments with evaporated SnPb(60/40) and AuSn(80/20) in vacuum always showed excellent wetting.
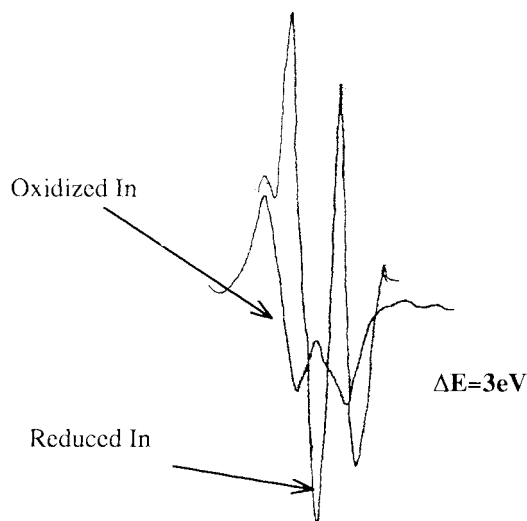
Fig. 11. Energy shift during *in situ* AES between In-oxide and metallic In, observed during reduction of In-oxide on eutectic InSn by H_2 at 250 °C.
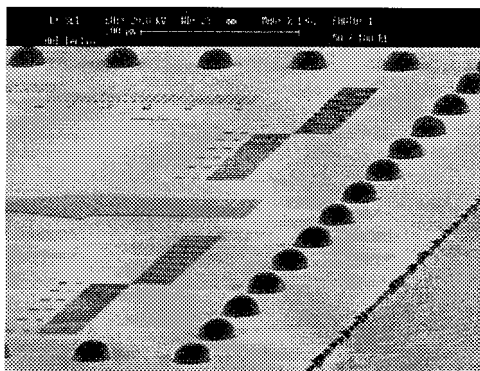

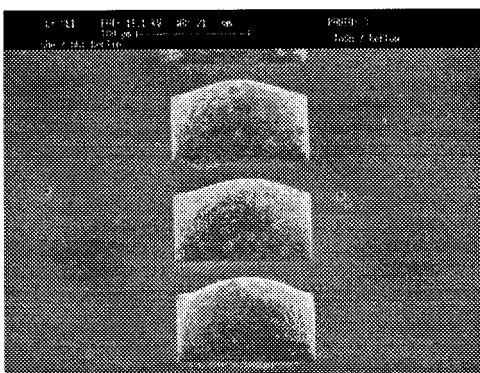Fig. 12. Reflow of SnPb(60/40) bumps in vacuum $\leq 10^{-1}$ Pa.

Fig. 13. Electroplated InSn(51.2/48.8) after reflow in vacuum ($p_{\mathrm{total}} = 10^{-4}$ Pa).

Nevertheless, the passive alignment of the samples was not achieved in the narrow tolerances which are needed, e.g., for the assembly of photonic devices. In that area, using pre-reflowed SnPb and AuSn solder bumps, deposited by evaporation, it was shown that the desired bonding results only were achieved with the use of H_2 as a safe flux substitute [15].
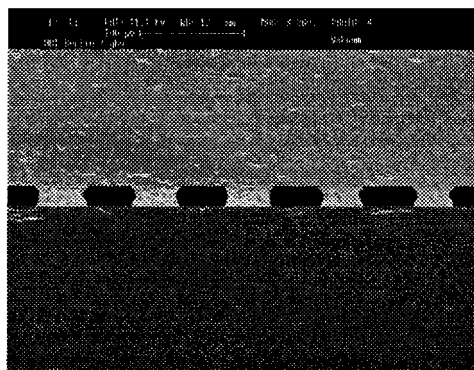

Fig. 14. Cross section of FC-bonded samples, bonded in vacuum ($p_{\mathrm{total}} = 10^{-4}$ Pa).
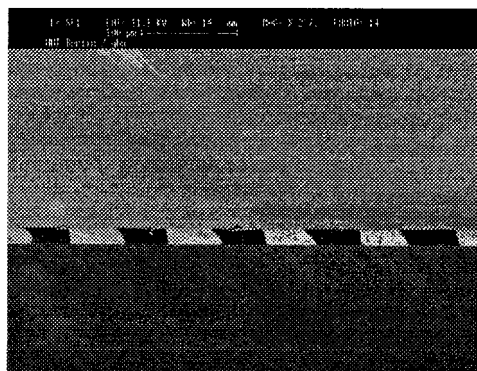

Fig. 15. Cross section of FC-bonded samples, bonded in vacuum ($p_{\mathrm{total}} = 10^{-4}$ Pa).

Figs. 14 and 15 show two cross sections of samples bonded in vacuum ($p_{\mathrm{total}} = 10^{-4}$ Pa): from Fig. 14 it can be seen, that the bump-shape of the reflown solder bumps partly remained intact. Fig. 15 shows the solder bumps still remain in their tilted position after bonding. Using evaporated and reflown SnPb(60/40) bumps the alignment was not in the tolerable range of 2 μm.

In contrast to that, bonding experiments at 250 and 320°C ($t \leq$ 2 min), carried out with H_2 as a reducing agent (p_{H_2}/p_{H_2O} values see Table II), using eutectic SnPb and AuSn bumps led to solder joints exhibiting cross-sections of a barrel shaped, symmetrical contour. With this new FC-bonding process an accuracy of 1.4 $\pm$ 0.8 μm ($n = 35$) was achieved.

The potential of H_2 to reduce oxides on solder bumps can be very effectively demonstrated using *in situ* observation during the self-alignment. The sequence of a FC-bonding process, using evaporated AuSn(80/20) solder bumps (see Fig. 16) clearly proves the applicability of H_2 for a fluxless and highly accurate FC-soldering process. After pre-alignment within an accuracy of $\sim$10 μm the samples were heated up to 320 °C. After the melting point of the solder was reached a spontaneous self-alignment occurred within the first few seconds. This self-alignment did nevertheless not exceed the accuracy of $\sim$5 μm. Then, after 120 s H_2 was introduced into the recipient in order to meet the required H_2/H_2O ratios for reduction of the Sn-oxide. The remaining oxide on the solder surfaces was reduced and the residual offset taken away within 60 s.
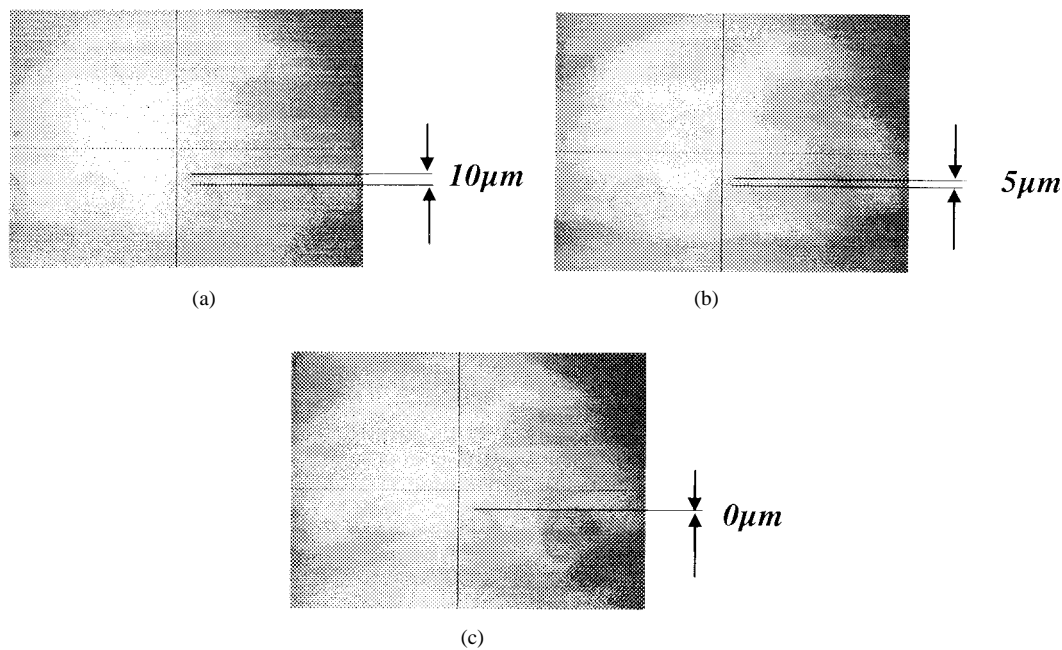
Fig. 16. Pictures, taken through a glass chip during FC-bonding. During bonding in vacuum self-alignment occurred, but only after injection of H_2 a complete overlap of chip metallization and bump footprint can be seen: (a) pre-alignment, $t = 0$ s, (b) alignment in vacuum (10^{-4} Pa), $t = 120$ s, and (c) alignment in vacuum $+H_2$, $t = 180$ s.

IV. CONCLUSION

This study of oxidation and reduction kinetics in conjunction with reflow and bonding experiments leads to important conclusions regarding fluxless soldering technologies:

1) On both solders a crystalline oxide is formed. For eutectic InSn and SnPb the oxide growth on the molten, metallic solder surface can be effectively reduced in vacuum.

2) The native oxide, grown on the solder surface during storage in ambient is an effective protection. For eutectic InSn and SnPb the oxide is most likely amorphous. In the case of SnPb(60/40) even during heat treatment above the eutectic temperature (200 and 250 °C) the oxide did not grow significantly. During storage at room temperature for three days and three months the oxide thickness was in both cases $\sim$3.5 nm. For InSn(51.2/48.8) a logarithmic growth of the oxide layer was observed which leads to 7–8 nm oxide after three days and three month storage at 22 °C, respectively. The eutectic AuSn was not characterized as thoroughly as the other solder materials but also here no deviation from the well known logarithmic scale growth is expected.

3) Reflow in vacuum showed good bump formation for all solder alloys, the surface of the InSn alloy being the least smooth. This might be due to the deposition technology, which was in the case of SnPb and AuSn evaporation whereas the InSn solder was electroplated. For AuSn(80/20) and also SnPb(60/40) even at elevated O_2 partial-pressures (10^{-1} Pa) a very good reflow of the evaporated solder to truncated spheres was observed.

4) Bonding experiments in vacuum using evaporated reflown SnPb(60/40) and AuSn(80/20) bumps showed excellent wetting. Also self-alignment of the samples after wetting occurred. The self-alignment depended on pre-alignment and the rate of reoxidation but never reached the quality which was observed using fluxes. The governing mechanism can be proven by the contour of the cross-sectioned solder joints and by *in situ* observation of the bonding process. Where the misalignment between the chip metallization and the pre-reflowed solder bumps has been moderate, the bump contour indicates, that large surface areas are still covered by the native oxide: the shape of the reflown bumps remained partly intact. Increasing misalignment between the parts led to tilted solder joints. Here the wetting of the opposite metallization has supported a larger change of the bump contour. In these cases self-alignment clearly could be observed. Nevertheless, the remaining oxide or reoxidation impeded self-alignment within the very close tolerances ($\leq$2 μm), needed, e.g., for the assembly of photonic devices.

5) In general the starting point of all soldering operations is a solder covered by its native oxide. This oxide, which for all investigated solder materials is very thin and stable can be taken away by H_2 during soldering in vacuum. The FC-bonding results, using evaporated and reflown AuSn(80/20) and SnPb(60/40) clearly prove the applicability of H_2 for a fluxless soldering process. Even high demands on alignment accuracy could be met with this process employing moderate temperatures and short heating cycles. In addition to the bonding results the potential of H_2 to reduce the oxides on eutectic InSn, SnPb, and AuSn solder could be proven by means of *in situ* AES measurements. Here the transition of the predominately oxidized species from oxidized to

the metallic state was monitored. Provided the necessary thermodynamic boundary conditions were met the reduction of the oxides occurred within 2 min.

REFERENCES

[1] S. M. Scheifers and C. J. Raleigh, "Effects of flux contamination on flip chip reliability," in *Proc. Sensors Electron. Packag. ASME,* 1995, Med-vol. 3/EEP-vol. 14, pp. 101–109.
[2] N. Koopman, S. Bobbio, S. Nangalia, and I. Bousaba, "Fluxless soldering in air and nitrogen," in *Proc. 43th ECTC,* 1993, pp. 595–604.
[3] T. Nishikawa, M. Ijuin, R. Satoh, Y. Iwata, M. Tamura, and M. Shirai, "Fluxless soldering process technology," in *Proc. 44th ECTC,* 1994, pp. 286–292.
[4] K. Markus, V. Duhler, D. Roberson, A. Cowen, M. Berry, and S. Nangalia, "Smart MEMS: Flip chip integration of MEMS and electronics," in *Proc. SPIE Smart Materials Conf.,* Feb. 1995, pp. 23–29.
[5] M. Heschel, J. F. Kubmann, S. Bouwstra, and M. Amskov, "Stacking technology for a space constrained microsystem," in *Proc. IEEE Workshop MEMS,* Heidelberg, Germany, Jan. 25–29, 1998, pp. 312–317.
[6] R. D. Deshmukh, M. F. Brady, R. A. Roll, and L. A. King, "Active atmosphere solder self-alignment and bonding of optical components," *Int. J. Microcirc. Electron.-Packag.,* vol. 16, no. 2, pp. 97–107, 1993.
[7] M. Itho, I. Yoneda, H. Hontnou, K. Fukushirna, and T. Nagahori, "Self-aligned packaging of multi-channel photodiode array module using AuSn solder bump flip-chip bonding," in *Proc. EuPac'96,* Jan. 31–Feb. 2, 1996, pp. 75–77.
[8] K. Boustedt, "Flip-chip with eutectic Pb/Sn bumps: A proposed process flow," in *Proc. ISHM Nordic Conf.,* 1996, pp. 116–122.
[9] H. Jiang, E. Jung, D. Lin, E. Zakel, and H. Reichl, "Failure mechanisms in underfill materials used for flip chip assembly on organic PCB," in *Proc. Micro Syst. Technol.,* 1996, pp. 111–117.
[10] R. D. Deshmukh, M. F. Brady, R. A. Roll, and L. A. King, "Active atmosphere solder self-alignment and bonding of optical components," *Int. J. Microcirc. Electron.-Packag.,* vol. 16, no. 2, pp. 97–107, 1993.
[11] H. Lau, *Solder Joint Reliability, Theory and Applications.* New York: VanNostrand, 1991.
[12] J. I. Ivankowits and S. W. Jacobs, "Atmosphere effects on the solder reflow process," in *Proc. SMTCON Technol.,* 1990, pp. 283–300.
[13] J. F. Kuhmann, H.-J. Hensel, and H.-G. Bach, "Flip chip investigations on the self-alignment of tin–lead solder," in *Proc. Eupac'96,* Essen, Germany, Jan. 31–Feb. 2, 1996, pp. 37–40.
[14] J. F. Kuhmann, H.-J. Hensel, D. Pech, P. Harde, and H.-G. Bach, "Self-aligned, fluxless flip-chip bonding technology for photonic devices," in *Proc. 46th ECTC,* May 28–31, 1996, pp. 1088–1092.
[15] J. F. Kuhmann, W. Pittroff, A. Preuβ, P. Harde, and T. Wirth, "Fluxless flip-chip bonding for the photonic assembly: Comparison between evaporated SnPb(60/40) and AuSn(80/20)," in *Proc. Microsystems'96,* Balin, Germany, Sept. 18–20, 1996, pp. 91–97.
[16] J. F. Kuhmann and D. Pech, "*In situ* observation of the self-alignment during FC-bonding under vacuum with and without H$_2$," *IEEE Photon. Technol. Lett.,* vol. 8, Dec. 1996.
[17] A. Preuss, B. Adolphi, and K. Drescher, "Oxidation of In-48Sn," *J. Electrochem. Soc.,* vol. 141, no. 10, pp. 2784–2788, 1994.
[18] J. F. Kuhmann, K. Maly, and T. Wirth, "Oxidation kinetics of liquid eutectic tin–lead solder under ambient and vacuum conditions," in *Proc. MicroMat'97 Conf.,* Berlin, Germany, Apr. 16–18, 1997, pp. 859–862.
[19] O. Knacke, O. Kubatschewski, and K. Hesselmann, *Thermochemical Properties of Inorganic Substances.* Berlin, Germany: Springer-Verlag, 1991.

Jochen F. Kuhmann received the degree in materials science, quality management, and electronic packaging from the Technical University of Berlin, Berlin, Germany in 1993 and the Ph.D. degree in fluxless and self-aligned flip-chip solder bump bonding for the photonic assembly from the Heinrich-Hertz-Institute, Berlin, Germany in 1996.

Since July 1996, he has been with Mikroelektronik Centret, Lyngby, Denmark, where he is developing stacking technologies for intelligent transducers together with industrial partners.

Andrea Preuss received the M.Sc. and Ph.D. degrees in material science from the Technical University of Dresden, Dresden, Germany, in 1986 and 1993, respectively.

She has worked in the development of processes and materials for integrated circuit metallization, especially for the back end processes like soldering. Her main interest involves different methods for material characterization like electron microscopy, electron spectroscopy, and X-ray diffraction.

Barbara Adolphi received the M.Sc. and Ph.D. degrees from the Department of Physics, Technical University of Dresden, Dresden, Germany, in 1971 and 1979, respectively.

She has worked in the area of surface analysis and from 1978 to 1986, she worked in the industrial research and development of Si-based nuclear radiation detectors. In 1986, she joined the Laboratory of Microelectronics and Microsystems, Technical University of Dresden. She has since worked in the area of surface analysis and development of materials and processes in microelectronics, especially the back end process.

Karsten Maly received the M.Sc. degree in materials science from the Technical University of Berlin, Germany, in 1997.

His fields of interest include metals and packaging technologies in microelectronics. He is currently with Sulzer Orthopedics Ltd., Berlin, Germany, where he is conducting failure mode analysis on hip and knee protheses.

Thomas Wirth received the degree in physics from the Department of Physics, Technical University of Dresden, Dresden, Germany, in 1975.

From 1975 to 1991, he worked for the Central Institute of Electron Physics, Academy of Sciences of the GDR, with surface analytical techniques to investigate plasma-wall interactions in nuclear fusion reactors (Tokamak) and semiconductor devices. He also prepared and analyzed Schottky as well as ohmic MESFET contacts. Since 1991, he has been with the Federal Institute of Materials Research and Testing, Berlin, Germany, where he is responsible for micro-area and surface analysis and scanning electron microscopy.

Werner Oesterle received the Ph.D. degree in materials science from the Technical University of Berlin, Berlin, Germany in 1981.

He began work at the Federal Institute of Materials Research and Testing, Berlin, Germany, as a Research Engineer. Since 1988, he has been Head of the Department for Electron Microscopy. Besides the characterization of thin film structures, his main fields of interest are deformation structures of metallic materials and material reactions at tribological contacts.

Wolfgang Pittroff received the M.Sc. degree in semiconductor electronics from the Leningrad Electrotechnical Uljanov Institute, Leningrad, Russia, in 1974 and the received the Ph.D. degree from the Ferdinand-Braun-Institut für Höchstfrequenztechnik, Berlin, Germany in 1984.

From 1974 to 1978, he was a Process Engineer in the Television Electronics Company, Berlin, Germany. From 1978 to 1991, he was with the Central Institute for Optics and Spectroscopy of the Academy of Sciences of the GDR where he first worked on electrical measurement techniques for laser diode structures and then on 1.5-mm semiconductor laser arrays. Since 1992, this work was continued with the newly founded Ferdinand-Braun-Institut für Höchstfrequenztechnik, Berlin. His research interests presently focus on mounting technologies for laser diodes.

Gerd Weyer received the Ph.D. degree from the Free University of Berlin, Berlin, Germany.

He is currently an Associate Professor of Physics at the Institute of Physics and Astronomy, University of Århus and Scientific Associate at CERN, Geneva. His specific interests are solid state physics of metallic and semiconducting materials and the application of nuclear methods utilizing radioactive isotopes.

Marco Fanciulli received the Laurea degree in nuclear engineering (with honors) from the Politecnico di Torino, Torino, Italy, in 1987 and the Ph.D. degree in applied physics from Boston University, Boston, MA in 1993.

From 1993 through 1997, he was an Assistant Professor at the Institute of Physics and Astronomy, Århus University, Denmark, where he is now an Associate Professor. His interests are in the study of semiconductors and intermetallic compounds using different methods such as Mossbauer spectroscopy, magnetic resonance, and deep level transient spectroscopy.